Electrochemical Behavior of p-Type Indium Selenide Single Crystal Electrodes in Dark and under Illumination

Kohei UOSAKI,* Susumu KANEKO, Hideaki KITA, and A. CHEVY†
Department of Chemistry, Faculty of Science, Hokkaido University, Sapporo 060
†Physique des Milieux très Condensés, Université Pierre et Marie Curie-Paris VI, 75230 Paris Cedex 05, France
(Received September 30, 1985)

The electrochemical behaviors of van der Waals face of p-InSe single crystal electrodes in 0.5M H_2SO_4 and 1M NaOH (1M=1 mol dm^{-3}) with and without illumination have been thoroughly investigated. In 0.5M H_2SO_4, relatively large cathodic dark current was observed and the onset potentials for the current in dark and under illumination were ca. −0.8 V (vs. Ag/AgCl) and ca. −0.5 V, respectively, at as-prepared electrode. The current seemed to be mainly due to hydrogen evolution reaction. The dark current decreased significantly and the photocurrent increased by removing surface steps. These results and impedance analyses show that the surface steps create surface states which act as recombination centers and mediators for charge transfer. Both the dark- and photocurrent onset potentials in 1M NaOH were more negative than those in 0.5M H_2SO_4 by ca. 0.5 V. The dark current was quite large and the photocurrent was small in 1M NaOH even after removing surface steps. By depositing Pt on p-InSe, the photocurrent onset potential shifted towards positive by several hundred mV. The reaction mechanism of photoelectrochemical hydrogen evolution was discussed by considering the above results.

One of the major difficulties in the photoelectrochemical energy conversion is the lack of stability of the semiconductor electrodes under illumination.[1] Many attempts were made to stabilize the electrodes[2] and to seek new electrode materials.[3]

Layered compound semiconductors are expected to have high stability as photoelectrodes.[4] Also, because there is no dangling bond, which creates surface states, at cleaved surface of these materials,[5] the surface recombination probability should be low that leads to high conversion efficiency. Although the photoelectrochemical characteristics of transition metal chalcogenides have been studied very extensively,[6] those of III—VI compound semiconductors are not well known. Indium selenide (InSe) has an ideal energy gap (1.1—1.3 eV[7]) for solar energy conversion devices[8] but only a few reports are available for this application.[9] The photoelectrochemical behavior of InSe was first reported by McCann very briefly.[10] Recently, Levy-Clement et al. reported basic electrochemical characteristics of InSe relatively in detail.[11]

In this paper, we report the thorough study of (photo)electrochemical hydrogen evolution reaction at van der Waals face of p-InSe single crystal.

Experimental

InSe single crystals used in this study were grown by the Bridgman method.[12] p-InSe was doped with Zn by 0.1%. Cleaved surface was always used as an electrode. An ohmic contact was obtained by an In–Zn alloy. Because of weak mechanical strength of the material, Ti plate was used as a support. After the ohmic contact was insured, silver conducting paste (Fujikura Kasei Co. Ltd., Dotite D-550) was used to fix the back side of the electrode to a Ti plate to which Cu wire was connected by using the conducting paste. Except the front face, all other parts were covered with epoxy resin and the electrode was then placed in a glass tubing.

Electrolyte solutions were prepared by using reagnt grade chemicals and water purified by Milli-Q water purification system (Millipore Corp.).

An ordinary three compartment cell with a Pyrex window was used for the measurements. A counter and a reference electrode were a Pt wire and a Ag/AgCl electrode, respectively. The electrode potential was controlled by using a potentiostat (Hokuto Denko, HA-501).

A 500W Xe lamp (Ushio Electric Co. Ltd., UXL-500D-0) with an IR absorbing filter (Toshiba, IRA-20) or a monochromator (Ritsu Oyo Kogaku, MC-25NP) was used as a light source for photocurrent-potential and photocurrent-wavelength relation measurements. The photocurrent-wavelength measurements were carried out with a constant light intensity. A 20 mW He–Ne laser (NEC Corp., GLG5700) with ND filters was used as a light source for the light intensity-photocurrent relation measurements. The intensity of the light was monitored by means of a light power meter (Anritsu Electric Co. Ltd., ML-94A with an MA-97A detector).

Impedance measurements were carried out in dark by using the potentiostat and a frequency response analyzer (NF Electronic Co. Ltd., S-5720B) which was controlled by a personal computer (NEC Corp., PC-8801) via GP-IB interface. In these measurements, a large Pt foil was used as a counter electrode to minimize the impedance due to the counter electrode.

Platinization of the electrode was performed either by dipping the electrode in a H_2PtCl_6 solution (20 mM, pH=4) for 1 min or by the electodeposition in the same solution at 0 V (vs. Ag/AgCl). In the latter case, the amount of Pt deposited was estimated from the charge passed during the deposition.

XPS spectra and visible and near-IR absorption spectra were obtained by using an ESCA-3 (VG Scienticific Ltd.) and a photospectrometer (Shimadzu Ltd., UV-365), respectively.

All the electrochemical measurements were carried out at room temperature after the electrolyte solution was deaerated by passing a purified He gas for at least 20 min.

Results

Spectroscopic Characterization. Layers of InSe were removed by adhesive tape and visible and near-IR spectra of this sample were taken against the adhesive tape without InSe layers as a reference. Figure 1 shows

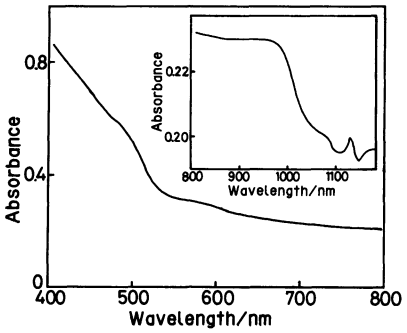

Fig. 1. Absorption spectra of InSe in visible region and in near IR region (inset).

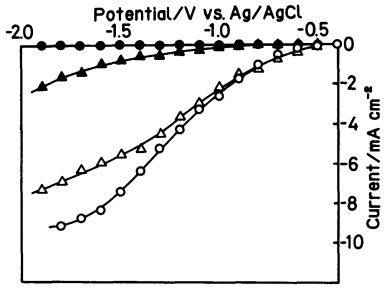

Fig. 2. The dark current (▲,●)- and photocurrent (△,○)-potential relations in 0.5 M H_2SO_4. ▲,△: As-prepared electrode. ●,○: Same electrode after removal of surface steps.

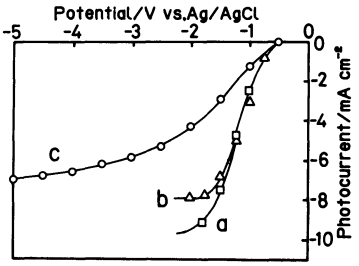

Fig. 3. The photocurrent-potential relations of three p-InSe samples in 0.5 M H_2SO_4. (a): Sample 1, (b): Sample 2, (c): Sample 3.

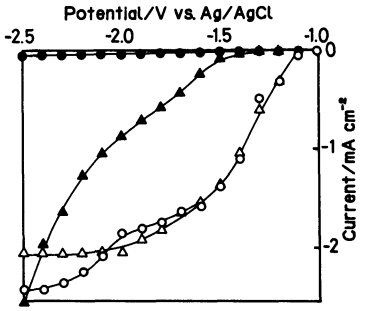

Fig. 4. The dark current (▲,●)- and photocurrent (△,○)-potential relations in 1 M NaOH. ▲,△: As-prepared electrode. ●,○: Same electrode after removal of surface steps.

the visible and near IR absorption spectra. The results were essentially in good agreement with those of Piccioli et al.[7b] with indirect absorption edge at ca. 1000 nm and direct absorption edge at ca. 500 nm. The peak around 1130 nm is considered to be due to exitons.[7b]

Peak energies of the XPS spectra of InSe surface due to In 3d peaks obtained without sputtering agree with those of In metal due to In 3d peaks with Ar^+ sputtering within experimental error, suggesting that indium exists as In(0) state and there is no noticeable indium oxide layer at InSe surface.

Current-Potential Relations with and without Illumination. Figure 2 shows typical current-potential relations of an as-prepared p-InSe electrode in 0.5M H_2SO_4 with and without illumination of light. Relatively large cathodic dark current was observed and while the dark current onset potential was ca. −0.8 V, the cathodic photocurrent was observed at potentials more negative than ca. −0.5 V. The current seemed to be mainly due to hydrogen evolution, since bubbles were observed at the electrode surface and no surface change was noticed after the measurements.

It has been known that the existence of steps at semiconductor electode surface, the van der Waals face of layered compounds in particular, affects the electrochemical behavior of the electrode both with and without illumination.[13] Although the electrode surface was prepared by removing steps with adhesive tape, there were still many steps on the as-prepared InSe clectrode. When the as-prepared electrode was anodically polarized, the dark anodic current due to the oxidation of the electrode was observed. The anodic dark current flowed preferentially through steps as regions near steps became red due to Se deposition.[14] After the Se deposition, the position of steps became more apparent and the removal of steps became easier. Thus, the most of the experiments reported in this work were carried out after the electrode was anodically polarized at 0.5 V (vs. Ag/AgCl) and the surface steps were removed as much as possible. Figure 2 also shows the current-potential relations of the same electrode but after the removal of steps. It is very clear from this figure that the dark current reduced significantly while the photocurrent increased by removing steps. The results reported by Levy-Clement et al. showed relatively large dark current, suggesting the existence of many surface steps.[11]

During the experiments, we noticed the electrochemical behavior differed from sample to sample quite significantly. Figure 3 shows the photocurrent-potential relations of three samples[15] used for the experiments. Although the photocurrents were observed at potentials more negative than ca. −0.5 V and saturated with the value of 8—10 mA cm^{-2} at all samples, the potentials at which the photocurrent showed saturation were different from sample to sample.

Figure 4 shows the current-potential relations in 1M

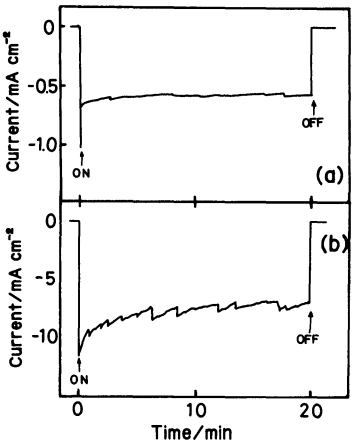

Fig. 5. Current-time relations of p-InSe in 0.5 M H_2SO_4 at (a) −1.0 V and (b) −2.0 V vs. Ag/AgCl. Current before illumination are taken as zero.

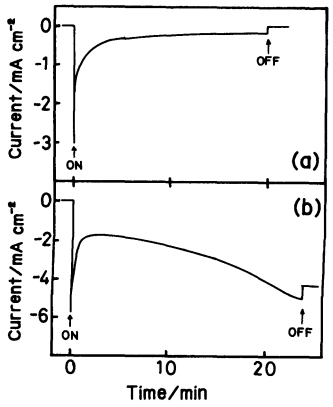

Fig. 6. Current-time relations of p-InSe in 1.0 M NaOH at (a) −1.5 V and (b) −2.5 V vs. Ag/AgCl. Current before illumination are taken as zero.

NaOH of the sample used in Fig. 2 with more and less surface steps. Both the dark and the photocurrent onset potential were more negative than those in 0.5M H_2SO_4 by ca. 0.5 V. These results contrast to the results of GaSe at which no pH dependence was observed.[16] In 1M NaOH, the dark current was quite large even with less surface steps and the photocurrent was small compared to the current in 0.5M H_2SO_4. After the measurements in 1M NaOH, white film was observed on the surface and the electrode swelled and was very easily broken.

Stability. The photocurrent was relatively constant and no significant change of the dark current was observed in 0.5M H_2SO_4 as shown in Fig. 5(a) and (b). The fluctuation of the current was mainly caused by hydrogen bubble which stack on and suddenly left from the electrode surface. On the other hand, in 1M NaOH the photocurrent decreased very quickly (Fig. 6(a) and (b)) and the dark current increased at strong negative bias (Fig. 6(b)). As was the case in the current-potential relation measurements, white film was formed and the electrode became mechanically very weak after the stability measurements in 1M NaOH.

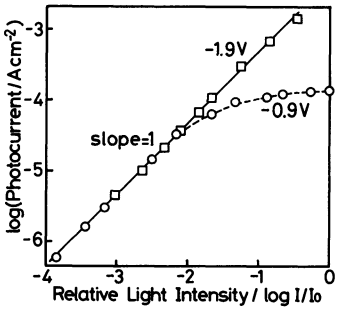

Fig. 7. Light intensity dependence of the photocurrent of p-InSe in 0.5 M H_2SO_4 at −0.9 V (○) and −1.9 V (□) vs. Ag/AgCl (I_o=1.41 mW cm^{-2}).

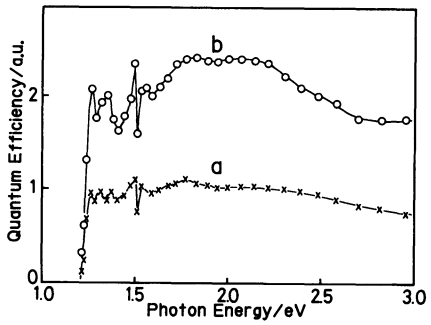

Fig. 8. The photocurrent action spectra of p-InSe in 0.5 M H_2SO_4. At −0.9 V (curve a) and −1.9 V (curve b) vs. Ag/AgCl.

Effect of Light Intensity on Photocurrent. Figure 7 shows the photocurrent-light intensity relations in 0.5M H_2SO_4 at −0.9 V and at −1.9 V. At −0.9 V at which the potential dependence of the photocurrent was large, the photocurrent increased linearly with light intensity as far as the intensity was not too strong but it tended to saturate at higher light intensity. On the other hand, at −1.9 V at which the photocurrent was almost independent of potential, the photocurrent increased lineary with the light intensity even at highest intensity employed in this study . Light intensity independent photocurent has been reported at various semiconductor electrodes.[17]

Quantum Efficiency Action Spectra. Since, as reported above, the quantum efficiency may be affected by light intensity, the quantum efficiency action spectra were obtained with constant light intensity for all measurements. Figure 8 shows the action spectra at −0.9 V and at −1.9 V. No significant shape difference between two spectra was observed. The bandgap energy obtained from these spectra (≈1.2 eV) is in good agreement with the absorption edge (cf Fig. 1).

Impedance Measurements. Figures 9 and 10 are the Cole-Cole plots of the impedance of p-InSe with many steps and with less steps, respectively, in 0.5M H_2SO_4. Although the real component increased with the decrease of the frequency in both cases, the frequency dependence of the imaginary component was

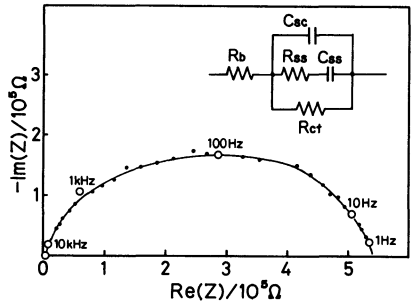

Fig. 9. Cole-Cole plot and the equivalent circuit of p-InSe electrode with many steps in 0.5 M H_2SO_4 without illumination of light. R_b and C_{sc} represent a bulk resistance and a space charge layer capacitance, respectively.

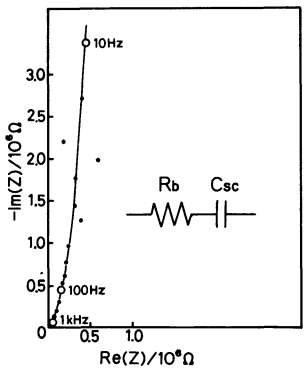

Fig. 10. Cole-Cole plot and the equivalent circuit of p-InSe electrode with many steps in 0.5 M H_2SO_4 without illumination of light. R_{ss} and C_{ss} are the resistance and capacitance of surface state, respectively, and R_{ct} is a charge transfer resistance.

quite different. While the absolute value of the imaginary component of p-InSe with many steps increased with the decrease of the frequency, reached the maximum at ca. 100 Hz and decreased with the decrease of the frequency, that of p-InSe with less steps increased monotonically with the decrease of the frequency.

The equivalent circuits for the former and the latter are also shown in Figs. 9 and 10, respectively.[18] Because of large dark current which leads to the sticking of hydrogen bubble on the electrode surface, the reproducibility of the impedance measurements was low and the potential dependence of the impedance was not determined at the electrode with many steps. The values of the space charge capacitance determined by analyzing the impedance results at various potentials in 0.5M H_2SO_4 with the equivalent circuit shown in Fig. 10 were used to obtain the Mott-Schottky plot of the electrode with less steps (Fig. 11). The flat band potential determined from the plot is +0.2 V (vs. Ag/AgCl). No reliable results were obtained in 1M NaOH due to continuous change of the electrode state.

Effect of Platinum Treatment. The photocurrent-potential relations in 0.5 M H_2SO_4 of p-InSe dip-treated in the H_2PtCl_6 solution and of p-InSe on which Pt was electrodeposited are shown in Fig. 12. In both cases, the photocurrent onset potential shifted towards positive by several hundred mV by Pt treatments. The saturated photocurrent was not affected by the treatments.

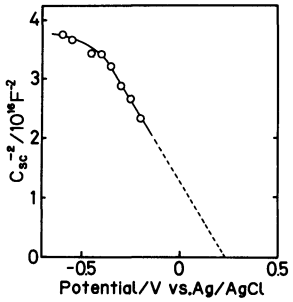

Fig. 11. The Mott-Schottky plot of p-InSe electrode with less steps in 0.5 M H_2SO_4.

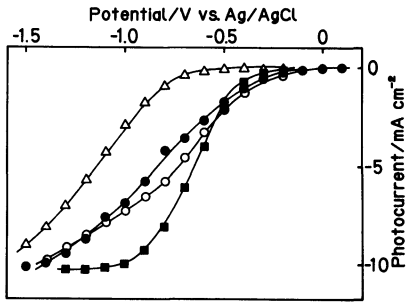

Fig. 12. The photocurrent-potential relations of p-InSe in 0.5 M H_2SO_4. △: Bare, ○: Dip-treated in 20 mM H_2PtCl_6 (pH=4) for 60 sec. ● and ■: Pt electrodeposited. Platinum was electrodeposited in 20 mM H_2PtCl_6 (pH=4) at 0 V vs. Ag/AgCl and the average thickness of Pt was estimated to be 2 Å (●) and 20 Å (■), respectively.

Discussion

pH-Potential Diagram (Pourbaix Diagram) and Stability. To examine the thermodynamic stability of InSe, the pH-potential diagram was constructed (Fig. 13). In Fig. 13, lines (1)—(10) represent the equilibrium reactions of the same numbers shown in Table 1. From the figure, it is confirmed that the red material deposited after the anodic polarization is Se. The white film observed on InSe surface after the (photo)-electrochcmical measurements in 1M NaOH solution must be indium, according to the figure. Although the stable region is wider in acidic solutions than in alkaline solutions, the big difference of the stability observed between these solutions experimentally cannot be explained simply by the thermodynamic data. Reaction (8) should be kinetically more favorable than reaction (6). There is also a possibility of intercalating reaction[22]

$$InSe + Na^+ + e^- \longrightarrow InSe(Na) \qquad (I)$$

Table 1. Equilibrium Reactions of InSe and the Corresponding Electrode Potentials

Reaction	Electrode Potential/V vs. NHE
(1) $In^{3+}+3/2H_2O=1/2In_2O_3+3H^+$	(pK=7.73)
(2) $In_2O_3+H_2O=2InO_2^-+2H^+$	(pK=−17.05)
(3) $In^{3+}+Se+3e^-=InSe$	E=0.233+0.0197 log[In^{3+}]
(4) $1/2In_2O_3+Se+3H^++3e^-=InSe+3/2H_2O$	E=0.386−0.0591 pH
(5) $InO_2^-+Se+4H^++3e^-=InSe+2H_2O$	E=0.721−0.0197 log[InO_2^-]−0.782 pH
(6) $InSe+2H^++2e^-=In+H_2Se$	E=−0.987−0.0295 p_{H_2Se}−0.0591 pH
(7) $InSe+H^++2e^-=In+HSe^-$	E=−1.129−0.0295 log[HSe^-]−0.0295 pH
(8) $InSe+2e^-=In+Se^{2-}$	E=−1.546−0.0295 log[Se^{2-}]
(9) $H_2Se=H^++HSe^-$	(pK=4.77)
(10) $HSe^-=H^++Se^{2-}$	(pK=14.01)

The thermodynamic values used for calculation are all taken from Ref. 19 for indium compounds and from Ref. 20 for selenium compounds except for $\Delta G_f^\circ(InSe)$=129.26 kJ·mol^{-1} which is taken from Ref. 21.

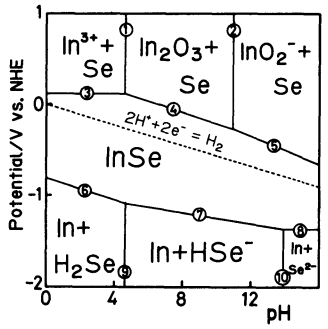

Fig. 13. The pH-potential diagram for the InSe-water system at 25 °C. Each line represents the equilibrium reaction of the same number shown in Table 1 with the following activity. For lines (1) and (3), [In^{3+}]=10^{-6}; for lines (2) and (5), [InO_2^-]=10^{-6}; for lines (6) and (9), p_{H_2Se}=10^{-6}; for lines (7), (9), and (10), [HSe^-]=10^{-6}; for lines (8) and (10), [Se^{2-}]=10^{-6}.

in 1M NaOH, as the mechanical strength of the electrode became very weak after the measurements.

The Reason for Irreproducible Current-Potential Relations. As shown in Fig. 3, the electrochemical behaviors were different from sample to sample. Particularly, the potentials at which the photocurrent showed saturation were different by as large as ≈3 V. In all cases, the photocurrent linearly increased with the potential at medium bias conditions and the resistances calculated from the linear portion by using ohmic law were 0.12 kΩ (sample 1), 0.13 kΩ (sample 2), and 0.50 kΩ (sample 3). The larger the resistance was, the more negative the potential at which the photocurrent saturated. The conductivity of InSe shows anisotropy and that perpendicular to the van der Waals face is relatively low.[23] Thus, the relatively large bulk resistance ⊥ the electrode surface causes large ohmic drop and the actual potential drop at the semiconductor/electrolyte interface (including within space charge layer) becomes low. The resistance difference among samples seemed to be due to the thickness difference.

Effect of Steps on the Electrochemical Behavior. As shown in Fig. 3, the dark current decreased significantly and the photocurrent increased by removing surface steps. The surface steps at which dangling bonds exist[24] certainly create surface states.[25] The results of current-potential relations can be explained by considering the existence of surface states at the electrode with many steps. Thus, the surface states act as recombination centers[26] and mediators for charge transfer,[27] resulting in smaller photocurrent and larger dark current at the electrode with many steps. The impedance analyses (Figs. 9 and 10) also support the above arguments. While the equivalent circuit for the electrode of less steps is simply a series combination of a bulk resistance, R_b, and a space charge capacitance, C_{sc}, the contribution of a surface state resistance, R_{ss}, a surface state capacitance, C_{ss}, and a charge transfer resistance, R_{ct}, should be taken into account in the case of the equivalent circuit for the electrode of many steps. Small R_{ct} is equivalent to a large dark current. By removing steps, the concentration of surface states becomes low and, therefore, C_{ss} becomes small and R_{ss} and R_{ct} become large, giving the equivalent circuit of the electrode of less steps.

The Mechanism for Photoelectrochemical Hydrogen Generation and Effect of Pt Modification. The photocurrent-potential and the photocurrent-light intensity relations at p-InSe in 0.5M H_2SO_4 provide information for the photoelectrochemical hydrogen generation mechanism. The hydrogen evolution reaction at p-type semiconductor under illumination proceeds by the following processes.[28]

(a) Bulk processes:

$$h\nu \longrightarrow p_v^+ + e_c^-, \quad (II)$$

$$e_c^- \longrightarrow (e_c^-)_s, \quad (III)$$

$$e_c^- + p_v^+ \longrightarrow \text{recombination}, \quad (IV)$$

where p_v^+ is the hole in the valence band and $(e_c^-)_s$ and e_c^- are the electrons in the conduction band at the surface and at other places, respectively.

(b) Surface processes:

$$(e_c^-)_s + H_3O^+ \longrightarrow H(a) + H_2O, \quad (V)$$

$$H(a) + (e_c^-)_s + H_3O^+ \longrightarrow H_2 + H_2O, \quad (VI)$$

$$H(a) + H(a) \longrightarrow H_2, \quad (VII)$$

$$(p_v^+)_s + H(a) + H_2O \longrightarrow H_3O^+, \quad (VIII)$$

$$(e_c^-)_s + (p_v^+)_s \longrightarrow \text{Surface recombination}, \quad (IX)$$

$$(e_c^-)_s + \square_{ss} \longrightarrow \boxed{e^-}_{ss},$$
$$\boxed{e^-}_{ss} + (p_v^+) \longrightarrow \square_{ss}, \quad (X)$$

where H(a) represents hydrogen atom adsorbed on the semiconductor, $(p_v^+)_s$ is the hole in the valence band at the surface, $\boxed{e^-}_{ss}$ is the occupied surface state, and $\square_{ss}$ is the unoccupied surface state. The step expressed in Eq. (X) is the surface recombination via surface state. The combination of step (V) and step (VIII) could be called the surface recombination via adsorbed hydrogen state. The rate determining step for the hydrogen evolution reaction must be different at potentials more positive than ca. −1.8 V where the photocurrent incrcased with the increase of cathodic bias but became independent of light intensity at relatively high intensity from that at potentials more negative than ca. −1.8 V where the photocurrent was almost independent of the potential but increased linearly with light intensity. In the latter case, the generation of electron-hole pair (step (IV)) is the rate determining srep.[29] This was verified by the fact that the platinization did not affect the saturation photocurrent. On the other hand, in the former case, the rate seems to be controlled by the surface processes. The disagreement of the flat band potential (≈0.2 V) and the photocurrent onset potential (≈−0.5 V) is due to the fact that the reactions (V)—(VII) are slow compared to reactions (VIII)—(X). The significant increase of the photocurrent in this potential region and the positive shift of the photocurrent onset potential by the surface modification with Pt which is known to accelerate the hydrogen evolution reaction in dark[30] (steps (V)—(VII)) again support this mechanism. Although the photoelectrochemical characteristics of p-InSe is improved much by Pt modification, the photocurrent onset potential is still relatively negative and, thus, the efficiency is small. Further improvement is required to reach the efficiency level of other metal modified semiconductor electrodes, e.g. p-InP.[31]

Prof. T. Yokokawa is acknowledged for the encouragement during the course of this work.

References

1) a) H. Gerischer, *J. Electroanal. Chem.*, **58**, 263 (1975); b) M. S. Wrighton, *Acc. Chem. Res.*, **9**, 303 (1979); c) A. Heller, *Acc. Chem. Res.*, **14**, 154 (1981); d) B. Parkinson, *Acc. Chem. Res.*, **17**, 431 (1984).

2) a) Y. Nakato, T. Ohnishi, and H. Tsubomura, *Chem. Lett.*, **1975**, 883; b) J. O'M. Bockris and K. Uosaki, *Energy*, **1**, 76 (1976); c) R. Noufi, D. Tench, and L. F. Warren, *J. Electrochem. Soc.*, **128**, 2596 (1981); d) L. Fornarini, F. Stirpe, and B. Scrosati, *J. Electrochem. Soc.*, **130**, 2184 (1983).

3) a) G. Betz, H. Tributsch, and S. Fiechter, *J. Electrochem. Soc.*, **131**, 640 (1984); b) A. Katty, B. Fotouhi, and O. Gorochov, *J. Electrochem. Soc.*, **131**, 2806 (1984); c) S. H. Pawar, S. P. Tamhankar, and C. D. Lokhande, *J. Electrochem. Soc.*, **132**, 261 (1985).

4) a) J. Gobrecht, H. Gerischer, and H. Tributsch, *Ber. Bunsenges. Phys. Chem.*, **82**, 1331 (1978); b) H. Tributsch, *Ber. Bunsenges. Phys. Chem.*, **82**, 169 (1978); c) H. Tributsch, *J. Electrochem. Soc.*, **125**, 1086 (1978).

5) W. Kautek, J. Gobrecht, and H. Gerischer, *Ber. Bunsenges. Phys. Chem.*, **84**, 1034 (1980).

6) H. Tributsch, *Far. Diss. Chem. Soc.*, **70**, 189 (1980).

7) a) J. C. Merle, R. Bartiromo, E. Borsella, M. Piacentini, and A. Savoia, *Solid State Comm.*, **28**, 251 (1978); b) N. Piccioli, R. Le Toullec, F. Bertrand, and J. C. Chervin, *J. Phys.*, **42**, 1129 (1981).

8) G. H. Hewig and W. H. Bloss, *Thin Solid Films*, **45**, 1 (1977).

9) a) A. Segura, A. Chevy, J. P. Guesdon, and J. M. Besson, *Solar Energy Mater.*, **2**, 159 (1979/1980); b) A. Segura, J. P. Guesdon, J. M. Besson, and A. Chevy, *Rev. Phys. Appl.*, **14**, 253 (1979); c) A. Segura, J. P. Guesdon, J. M. Besson, and A. Chevy, *J. Appl. Phys.*, **54**, 876 (1983).

10) J. F. McCann and J. Pezy, *J. Electrochem. Soc.*, **128**, 1735 (1981).

11) a) C. Levy-Clement, N. Le Nagard, O. Gorochov, and A. Chevy, *J. Electrochem. Soc.*, **131**, 790 (1984); b) C. Levy-Clement and B. Theys, *J. Electrochem. Soc.*, **131**, 1300 (1984); c) R. Tenne, B. Theys, J. Rioux, and C. Levy-Clement, *J. Appl. Phys.*, **57**, 141 (1985).

12) A. Chevy, A. Kuhn, and M.-S. Martin, *J. Cryst. Growth*, **57**, 118 (1977).

13) a) H. J. Lewerenz, H. Gerischer, and M. Lübke, *J. Electrochem. Soc.*, **131**, 100 (1984); b) W. Kautek, H. Gerischer, and H. Tributsch, *Ber. Bunsenges. Phys. Chem.*, **83**, 1000 (1979).

14) See the pH-potential diagram in the discussion section.

15) All samples were taken from the same crystal.

16) H. Gerischer, J. Gobrecht, and J. Turner, *Ber. Bunsenges. Phys. Chem.*, **84**, 596 (1980).

17) a) K. Uosaki and H. Kita, *Solar Energy Mater.*, **7**, 421 (1983); b) K. Rajeshwar, *J. Electrochem. Soc.*, **129**, 1003 (1982).

18) M. Tomkiewicz, *J. Electrochem. Soc.*, **126**, 2220 (1976).

19) V. V. Losev and A. I. Molodov, "Encyclopedia of Electrochemistry of the Elements," ed by A. J. Bard, Marcel Dekker, New York (1975), Vol. VI, p. 2.

20) S. I. Zhdarov, "Encyclopedia of Electrochemistry of the Elements," ed by A. J. Bard, Marcel Dekker, New York (1975), Vol. IV, p. 362.

21) I. Barin and O. Knacke, "Thermochemical Properties of Inorganic Substances (Supplement)," Springer-Verlag, Berlin, Heidelberg and New York (1977), p. 312, p. 323, and p. 352.

22) H. Tributsch, *Appl. Phys.*, **23**, 61 (1980).

23) R. W. Damon and R. W. Redington, *Phys. Rev.*, **96**, 1498 (1954).

24) R. M. A. Lieth, "Physics and Chemistry of Materials

with Layered Structure," ed by R. M. A. Lieth, D. Reidel Pub. Co., Dordrecht-Holland (1977), Vol. I, p. 225.

25) R. H. Wilson, *J. Appl. Phys.*, **48**, 4292 (1977).

26) J. I. Pankove, "Optical Processes in Semiconductor," Dover Pub. Inc., New York (1971), p. 353.

27) P. Salvador and C. Gutierrez, *Surface Science*, **124**, 398 (1983).

28) K. Uosaki and H. Kita, *J. Electrochem. Soc.*, **128**, 2153 (1983).

29) a) J. A. Baglio, G. S. Calabrese, D. J. Harrison, E. Kamieniecki, A. J. Ricco, M. S. Wrighton, and G. D. Zoski, *J. Am. Chem. Soc.*, **105**, 2246 (1983); b) M. Gronet and N. S. Lewis, *J. Phys. Chem.*, **88**, 1310 (1984).

30) A. J. Appleby, M. Chemla, H. Kita, and G. Bronoël, "Encyclopedia of Electrochemistry of the Elements," ed by A. J. Bard, Marcel Dekker, New York (1982), Vol. IX, Part A, p. 383.

31) a) K. Uosaki and H. Kita, *Chem. Lett.*, **1984**, 301; b) A. Heller, E. Aharon-Shalom, W. A. Bonner, and B, Miller, *J. Am. Chem. Soc.*, **104**, 6942 (1982).